CHAPTER IV

INTERPRETATION OF THE ABSORPTION AND CIRCULAR DICHROISM SPECTRA OF THE OPTICALLY ACTIVE $K_3Pr_2(NO_3)_9$ SINGLE CRYSTAL

IV.1. INTRODUCTION

In this chapter we present a model calculation on optical activity to correlate the rotational strengths for different CF transitions of anhydrous $K_3Pr_2(NO_3)_9$ single crystal, experimentally obtained by Chatterjee[12] . Sen et al[69,130] developed a theoretical model to calculate the rotational strength for optically active lanthanide crystals. They did extensive studies on lanthanide dyglycolate (Ln.DG.) crystals. They calculated the magnetic dipole transition moment and the electric dipole transition moment considering the component to component transition of the CF states. They used the Judd-Ofelt mechanism to calculate the lanthanide intensities. Later Richardson and Faulkner[68] developed an elaborate theoretical model which takes into account in addition to 'static' contribution the 'dynamic' ligand polarization contribution to the lanthanide electric dipole moment. The details of the static and Dynamic contribution to the electric dipole moment has been discussed in chapter II. In collaboration with Chatterjee and Chowdhury[131] we tried to fit the relative change in sign of the theoretical $\frac{R_K}{D_K}$ (D_K is the dipole strength which is the sum of the squares of the absolute values of all the dipole moments) with the experimental one. The values of $\frac{R_K}{D_K}$ for the K-th band were obtained from experiment by Chatterjee . Our attempt is to see how far our theoretical model can explain the experimental results i.e. the CF spectra and the CD spectra.

The purpose of the present chapter is to see: (1) how far the model is successful in predicting the relative sign and order of magnitude of rotational strengths of our anhydrous praseodymium double nitrate crystal; (2) a comparative study between the results obtained from the best fitted CF parameters (emperical) and that obtained from the theoretical parameters ($\equiv A_{kq}$(total), which is the sum of point charge and polarizability contributions); (3) whether we can evaluate a best set of parameters which can explain simultaneously the all observed CF levels and the relative change in sign of $\frac{R_K}{D_K}$ of the CD spectrum.

IV.2. A BRIEF ACCOUNT OF THE EXPERIMENT

The experimental data (i.e. both the optical absorption spectra and the CD spectra) were obtained by Chatterjee using Cary 17D and JASCO 500 at room temperature and upto $20^{\circ}K$. They are reproduced in table IV.3 .

IV.3. CRYSTAL STRUCTURE

The crystal is cubic with the space group $P4_32_12$. The four body diagonals are the four three-fold axes. Eight RE-ions, having identical environments occupy the eight corners of the cube. The site symmetry of a RE ion is a twelve

coordinated polyhedron; the twelve oxygens come from six nitrate groups. The actual symmetry is C_3 which makes each unit optically active[132] (see Fig. IV.1) .

IV.4. METHOD OF CALCULATION

We can divide our calculation into three parts: In the first part we tried to calculate the various theoretical CF levels and their corresponding wave functions with some set of CF parameters. During our CF calculations we have taken the full J-mixing into consideration. Then in the second part we have calculated the electric dipole transition moment and the magnetic dipole transition moment and in each case the component to component CF transition was taken into account. Finally in the last portion of our calculation we have calculated the rotational strength (R_K) for different transitions. Now we shall discuss the calculations in details.

IV.4(a) CRYSTAL FIELD CALCULATIONS

The effective Hamiltonian of Pr^{3+} in a crystal assuming a C_3 site symmetry is given by

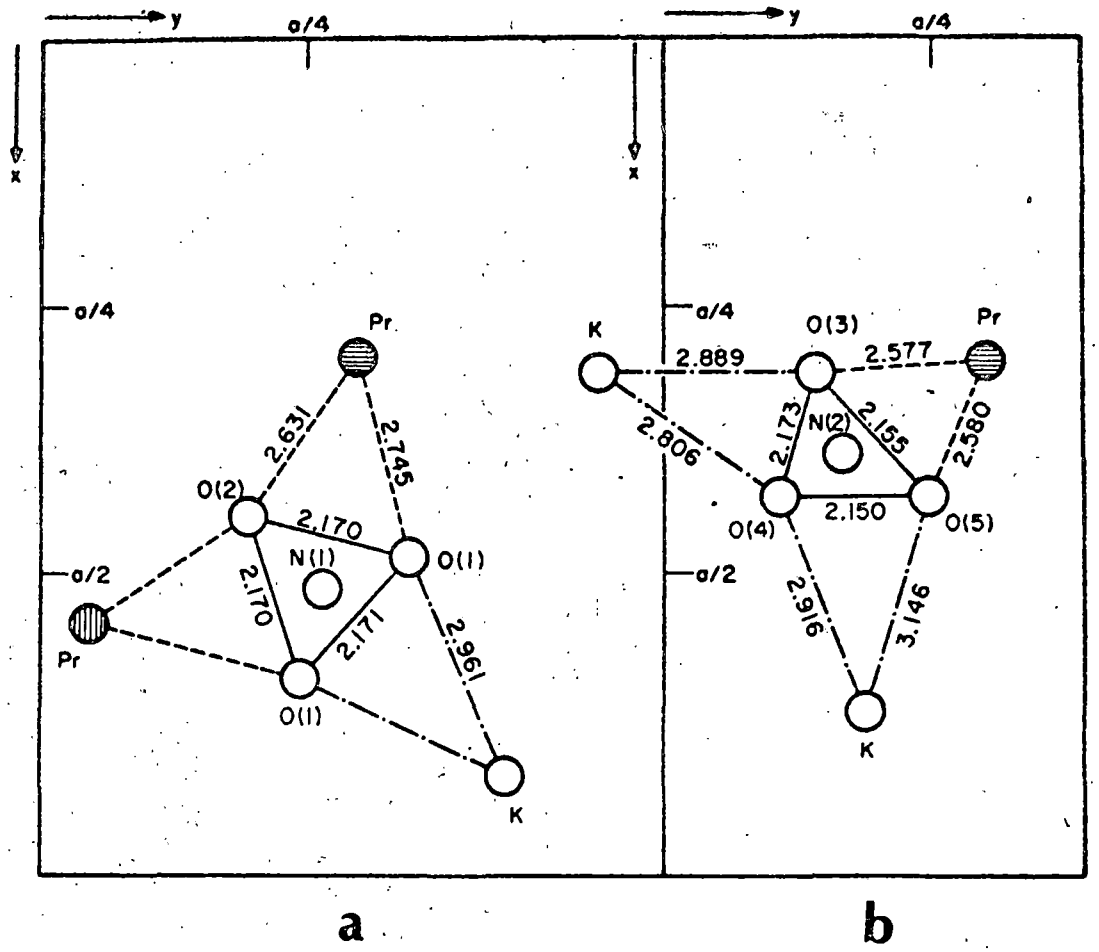

Fig. IV.1. Projection of "A" -type (a) and "B" -type (b) configurations, on the xy plane of $K_3Pr_2(NO_3)_9$.

$$\mathcal{H}_{eff} = \sum_{i<j} \frac{e^2}{r_{ij}} + \zeta \sum_i \underset{\sim}{l}_i \cdot \underset{\sim}{s}_i + A_{20}U_0^{(2)} + A_{40}U_0^{(4)} + A_{60}U_0^{(6)}$$

$$+ A_{66}(U_6^{(6)} + U_{-6}^{(6)}) + A_{43}(U_3^{(4)} - U_{-3}^{(4)}) + A_{63}(U_3^{(6)} - U_{-3}^{(6)})$$

$$+ iA'_{43}(U_3^{(4)} + U_{-3}^{(4)}) + iA'_{63}(U_3^{(6)} + U_{-3}^{(6)}) + iA'_{66}(U_6^{(6)} - U_{-6}^{(6)})$$

where A_{kq} and A'_{kq} are the real and imaginary part of the CF parameters in the tensor operator form. And $U_q^{(k)} = r^k Y_k^q$ is an irreducible tensor operator of rank k having q-th component.

The matrix elements of $\mathcal{H}_{eff}$ is constructed in a basis of states represented by $|UvSLJM\rangle$ (see chapter II). All states belonging to the different multiplet terms $^3P\,^3F\,^3H\,^1S\,^1D\,^1G\,^1I$ have been taken into consideration for the representation of the above matrix and it turns out to be a 91x91 matrix. The matrix element of the electrostatic part is obtained by a trial method by solving the Spedding's[79] matrix with a guess value of ζ so that it reproduces the free-ion energies given by Dieke[65]. The spin-orbit matrix elements for $4f^2$ configuration is given by Spedding[79]. We take those values. The value of ζ was determined by a trial procedure. The matrix element of $U_q^{(k)}$ is obtained by the tensor operator technique mentioned earlier in chapter II. Thus the 91x91 matrix is set up. But due to the crystal symmetry the whole matrix splits up into 2 matrices of dimension 30x30 (crystal quantum number $\bar{\mu} = \pm 1$) and one matrix of dimension 31x31 ($\bar{\mu} = 0$). Now one thing should be pointed here that the expansion of C_3 crystal field potential

contains both the 'C' term (real coefficient) and the 'S' term (imaginary coefficient) in the CF parameters.[133] The three CF parameters A'_{43} , A'_{63} and A'_{66} are coming from 'S' term. A'_{43} , A'_{63} and A'_{66} are individually real parameters. So iA'_{43}, iA'_{63} and iA'_{66} will be the crystal field parameters which are purely imaginary. Since the CF potential is always real so we take the combination of $U_3^{(4)}$ and $U_{-3}^{(4)}$; $U_3^{(6)}$ and $U_{-3}^{(6)}$ and $U_6^{(6)}$ and $U_{-6}^{(6)}$ in the last three combinations of CF interaction in such a way that the combination gives an imaginary i which on multiplication with iA'_{kq} parameters makes the CF interaction real. But according to the choice of our basis states the matrix element of the CF interaction part will be complex here. So this makes the three matrices complex. But still the whole matrix remains hermitian. One can solve the 3 above matrices by a direct complex matrix diagonalisation procedure. The same diagonalization can also be done by diagonalizing a real matrix in which the dimension of the whole matrix is made double of the original matrix. The detailed procedure has been described by Wilkinson[134] and we use the technique. So we have to diagonalize 2 matrices ($\bar{\mu} = \pm 1$) of dimension 60x60 and one matrix of dimension 62x62. During the diagonalisation of the matrix, the initial guess value of the different CF parameters were obtained as follows: A_{20} parameter was estimated from $^3P_1$ splittings, A_{40} and A_{43} parameters from $^1D_2$ splitting keeping A_{43}/A_{40} ratio as

obtained from point charge model. A_{60} , A_{63} and A_{66} parameters were guessed from the overall splittings of partially resolved $^3F_3$, $^3F_4$ and $^1G_4$ spectrum. The initial guess parameters A'_{43} , A'_{63} and A'_{66} were chosen directly from charge + polarizability contribution of the CF parameters (see chapter II). A complete computer program was then developed in which the CF matrix elements were automatically generated and then added up with SO and ES contribution and then the three matrices were diagonalized individually giving the different CF states and the corresponding energies. This takes into account the full J-mixing and also the intermediate coupling scheme which has already been discussed in chapter III. Starting with the guess value of the CF parameters we made an exhaustive trial method to see for which set of parameters the CF levels give the best fit with the experimental levels. The similar diagonalization was done with the parameters obtained from point charge + polarizability (theoretical) contribution. The two results were used to have a comparative study.

IV.4(b). CALCULATION OF THE MAGNETIC DIPOLE TRANSITION MOMENT AND THE ELECTRIC DIPOLE TRANSITION MOMENT

The contribution of the magnetic dipole transition moment between the different CF states was calculated using the computer diagonalised CF states and following the

appropriate selection rules for magnetic dipole transition (see chapter II). None of the transitions which we are considering, are directly magnetic dipole allowed but still the CF states contribute to the magnetic dipole intensity by mixing states of different J . The magnetic dipole moment calculation was done both for our fitted (emperical) CF parameters and also with the theoretical parameters independently. The details of the calculation of the magnetic dipole moment is given in chapter II.

The electric dipole transition moment arises in the $f^N \rightarrow f^N$ transitions by mixing with the odd parity states through the odd CF parameters, where

$$V = \sum_{t} A_{tp} D_p^{(t)}, \text{ with t odd .}$$

In the C_3 potential the allowed terms are $A_{3\pm3}$, $A_{5\pm3}$ and $A_{7\pm3}$. Foulkner and Richardson[68] gave a nice looking expression for the calculation of electric dipole transition moment both for static and the dynamic parts (see chapter II). The expression does not need the explicit values of odd CF parameters. We use their expressions for calculating the static and the dynamic contributions of the electric dipole moment and finally they were added up. While calculating the electric dipole moment we always consider the CF component to component transition. The electric dipole transition moment was calculated again with two sets of CF states (one is obtained from the emperical CF parameters and the other is obtained from the theoretical CF parameters).

The process for computing the magnetic dipole moment and the electric dipole moment was made in two separate computer programs.

IV.4(c). CALCULATION OF THE ROTATIONAL STRENGTH

The rotational strength (R_K) for a transition a → b is given by[67] the dot product

R_K = Imaginary part $\langle a|p|b\rangle . \langle b|m|a\rangle$

p and m are the electric and the magnetic dipole moment operators. We have already discussed how to obtain the contribution of the electric dipole moment and the magnetic dipole moment. As the CF states are complex for our system so the contribution of both the electric dipole moment and the magnetic dipole moments have real and the imaginary parts simultaneously. While calculating the rotational strength we need only the imaginary part of the product of electric dipole moment and the magnetic dipole moment. So in our case we can write the rotational strength as follows :

R_K = (Imaginary part of $\langle a|p|b\rangle$).(real part of $\langle a|m|b\rangle$) + (Real part of $\langle a|p|b\rangle$)x(Imaginary part of $\langle a|m|b\rangle$). The product of the total electric dipole moment and the magnetic dipole moment which has been calculated for the local axis system of each unit, was then re-expressed in terms of cubic

axis system and summed over the eight RE ions of the unit cell. It may be pointed out that the two ions located on opposite sides of any body diagonal of the cube are rotationally related (space group $P4_32$) and their contributions are added instead of cancelling. These are then compared with the experimental rotational strengths.

IV.5. RESULTS AND DISCUSSIONS

In the table IV.1 we have presented the values of ζ, $\langle r^2 \rangle$, $\langle r^4 \rangle$, $\langle r^6 \rangle$, $\overline{\alpha_L}$, q_L and C.I. parameters $\Xi_t(t,\lambda)$ which we have used in our calculations. The different set of CF parameters are presented in table IV.2 . Table IV.3 contains the different stark splitting and different $\frac{R_K}{D_K}$ obtained from experiment and from two sets of CF parameters. Where D_K is the dipole strength of the K-th band and it can be obtained theoretically by summing over the squares of all the dipole moments (i.e. both the electric and the magnetic dipole moments). The contribution of magnetic dipole moment is very small and hence the squares of this is again very small so we can neglect this safely from D_K . Since due to complex wave functions we have both the real part and the imaginary part of the electric dipole moment and the magnetic dipole moment, we can write

D_K = (Real part of the electric dipole moment)^2
+ (Imaginary part of the electric dipole moment)^2 .

We first tried to fit the experimental CF levels by adjusting the CF parameters. This was done by a trial procedure. The same CF level calculations were done by theoretical parameters alsp. In table IV.3 we have given the different stark splitting obtained for $^1D_2$, $^3P_0$, $^3P_1$ and $^3P_2$ manifold both from experiment and from our calculations. We find that overall stark splitting of the CF levels obtained from emperical parameters are in good agreement with the experimental findings. On the other hand the same thing obtained from theoretical parameters are significantly off from the experimental findings. So one may expect that the emperical CF parameters will give a better fitting with the experimental $\frac{R_K}{D_K}$ than that obtained from theoretical parameters. For a comparative study we have placed the experimental $\frac{R_K}{D_K}$ together with the theoretical $\frac{R_K}{D_K}$ (obtained both from emperical CF parameters and theoretical parameters) in table IV.3 . The results show that the theoretical values of $\frac{R_K}{D_K}$ are always higher in magnitude than the experimental ones. Specially some $\frac{R_K}{D_K}$ due to emperical set of CF parameters give very large values. Now, regarding the signs of $\frac{R_K}{D_K}$ we observe the following things :

In case of $^3H_4 \longrightarrow {}^1D_2$ transition the $\frac{R_K}{D_K}$ values for the theoretical parameters are as follows, out of four resolved

transitions all the four have the positive signs but in the experimental $\frac{R_K}{D_K}$ we have two are positive and two are negative. On the other hand $\frac{R_K}{D_K}$ obtained from emperical CF parameters gave a slight improvement in relative sign with the experimental findings. For the transition $^3H_4 \rightarrow {}^3P_0$ both the absolute and relative sign of $\frac{R_K}{D_K}$ obtained from theoretical CF parameters exactly match with the experiment. On the other hand only the relative sign of $\frac{R_K}{D_K}$ obtained from fitted set match with the experiment. For the fully resolved $^3H_4 \rightarrow {}^3P_1$ transitions we find that the signs of three experimental $\frac{R_K}{D_K}$ are positive and one is negative. The same results due to theoretical parameters show that the sign of three $\frac{R_K}{D_K}$ are positive and one is negative. We also find that the absolute sign of $\frac{R_K}{D_K}$ for two component to component transitions in both the above two-cases exactly match but the rest two transitions do not match exactly. For theoretical parameters we find that the relative sign of $\frac{R_K}{D_K}$ for last three consicutive transitions match with the experiment, but one component to component transition does not match at all.

In case of $^3H_4 \rightarrow {}^3P_2$ transition, the absolute and relative sign of $\frac{R_K}{D_K}$ with theoretical parameters exactly matches with the experiment, whereas in case of emperical parameters we succeed only in two.

So comparing the results obtained from theoretical parameters and the emperical parameters we conclude that optical activity calculation with the theoretical CF parameters is a better proposition for intensity matching than that with emperical CF parameters.

Table IV.1.

Values for Praseodymium ion Parameters

ζ_{so}/cm^{-1}	730
$\bar{\alpha}_L/A^3$	0.45
q_L/e.s.u.	-4.8×10^{-10}
$\langle r^2 \rangle/m^2$	3.04×10^{-21}
$\langle r^4 \rangle/m^4$	2.21×10^{-41}
$\langle r^6 \rangle/m^6$	3.45×10^{-61}
$H(1,2)/m^2J^{-1}$ *	-1.78×10^{-3}
$H(3,2)/m^4J^{-1}$	1.54×10^{-23}
$H(3,4)/m^4J^{-1}$	1.75×10^{-23}
$H(5,4)m^6J^{-1}$	-1.27×10^{-43}
$H(5,6)/m^6J^{-1}$	-5.45×10^{-43}
$H(7,6)/m^8J^{-1}$	4.54×10^{-63}

* $H(t,\lambda)$ —— : are the configuration interaction parameters.

Table IV.2

Values of Crystal field parameters (even ranked) for anhydrous and hydrated double nitrate single crystal.

A_{kq}	Values from Point charge + Polarizability model in cm^{-1}	Emperical parameters for $K_3Pr_2(NO_3)_9$ in cm^{-1}	Emperical parameters[124] for $Pr_2Zn_3(NO_3)_{12}\cdot 24H_2O$ in cm^{-1}
A_{20}	+72.3	+150	+191
A_{40}	-141.3	-107	-181
A_{60}	+96.7	+1296	+1022
A_{43}	+368.7	+202	±160
A_{63}	+241.7	+810	±2294
A_{66}	-191.0	+1755	-941
A'_{43}	+139.7	+89	-
A'_{63}	-85.0	+615	-
A'_{66}	+23.3	+203	-

Table IV.3.

Comparison of experimental, emperical and calculated $\frac{R_K}{D_K}$'s of $K_3Pr_2(NO_3)_9$

Transitions	Experimental results		Results with emperical CF parameters			Results with Theoretical (Point charge+Polarizability) CF parameters		
	Stark splitting in cm^{-1}	$\frac{R_K}{D_K} \times 10^4$	Stark splitting in cm^{-1}	Assignment of transition	$\frac{R_K}{D_K} \times 10^4$	Stark splitting in cm^{-1}	Assignment of transition	$\frac{R_K}{D_K} \times 10^4$
	0	+12.1	0	A→A	-20456.0	0	A→1E	+2.8
	61	-13.5	15	A→1E	+21.25	4	E→1E	+100.52
$^3H_4 \rightarrow {}^1D_2$	109	+6.12	61	E→A	+11.5	45	A→A	+190.6
			76	E→1E	+1205.10	50	E→A	+51.94
	152	-10.22	128	A→2E	-76.2	114	A→2E	+107.13
			189	E→2E	+452.60	118	E→2E	+201.5
$^3H_4 \rightarrow {}^3P_0$	0	+1.65	0	A→A	-3016.5	0	A→A	+21.08
	59	-0.93	60	E→A	+33.5	4	E→A	-137.0
$^3H_4 \rightarrow {}^3P_1$	0	+4.46	0	A→A	+45.9	0	A→A	+567.15
	32	+0.57	32	A→E	-164.6	5	E→A	+68.67
	59	-0.84	61	E→A	+68.07	16	A→E	+14.67
	96	+1.18	92	E→E	-1718.35	21	E→E	-193.6
$^3H_4 \rightarrow {}^3P_2$	0	+3.1	0	A→1E	-7.0	0	A→1E	+2.94
	53	-2.17	39	A→2E	-1.6	5	E→1E	-174.06
			61	E→1E	-10204.54	22	A→A	-16.86
			80	A→A	-2146.8	24	A→2E	-20.97
	106	-2.28	100	E→2E	-8125.66	27	E→A	+5.93
			141	E→A	+345.4	29	E→2E	-106.19